Mechanics and Mechanical Engineering
Vol. 11, No 1 (2007) 129–157

Inclined Load in Micropolar Thermoelastic Medium Possesing Cubic Symmetry with One Relaxation Time

Rajneesh Kumar and Praveen Ailawalia
Department of Mathematics, Kurukshetra University
Kurukshetra, Haryana, INDIA, 136119

Praveen Ailawalia
Department of Mathematics, Institute of Engineering and Emerging Technologies,
Makhnumajra, Baddi, Distt. Solan, H.P, INDIA, 173205

Received (10 October 2006)
Revised (15 March 2007)
Accepted (8 May 2007)

The analytic expressions for the displacements, microrotation, stresses and temperature distribution on the free surface of micropolar thermoelastic medium possessing cubic symmetry as a result of inclined load have been obtained. The inclined load is assumed to be a linear combination of a normal load and a tangential load. The Laplace and Fourier transforms have been employed to solve the problem. A special case of moving inclined load has been deduced by making the appropriate changes. The variations of the displacements, microrotation, stresses and temperature distribution with the horizontal distance have been shown graphically for both the problems.

Keywords: Micropolar, thermoelastic, cubic symmetry, inclined load, Laplace and Fourier transforms

1. Introduction

The classical uncoupled theory of thermoelasticity predicts two phenomena not compatible with physical observations. First, the equation of heat conduction of this theory does not contain any elastic terms, second, the heat equation is of a parabolic type, predicting infinite speeds of propagation for heat waves.

Biot [1] introduced the theory of coupled thermoelasticity to overcome the first shortcoming. The governing equations for this theory are coupled, eliminating the first paradox of the classical theory. However, both theories share the second shortcoming since the heat equation for the coupled theory is also parabolic.

Two generalizations to the coupled theory were introduced. The first is due to Lord and Shulman [24] who introduced the theory of generalized thermoelasticity with one relaxation time by postulating a new law of heat conduction to replace the

classical Fourier law. This new law contains the heat flux vector as well as its time derivative. It contains also a new constant that acts as a relaxation time. The heat equation of this theory is of the wave-type, ensuring finite speeds of propagation for heat and elastic waves. The remaining governing equations for this theory, namely, the equations of motion and constitutive relations remain the same as those for the coupled and uncoupled theories. The second generalization to the coupled theory of thermoelasticity is what is known as the theory of thermoelasticity with two relaxation times or the theory of temperature-rate-dependent thermoelasticity. Műller [26], in a review of the thermodynamics of thermoelastic solids, proposed an entropy production inequality with the help of which he considered restrictions on a class of constitutive equations. A generalization of this inequality was proposed by Green and Laws [7]. Green and Lindsay [8] obtained another version of the constitutive equations. These equations were also obtained independently and more explicitly by Suhubi [30]. This theory contains two constants that act as relaxation times and modify all the equations of the coupled theory, not only the heat equation. The classical Fourier's law of heat conduction is not violated if the medium under consideration has a center of symmetry.

The linear theory of micropolar thermoelasticity was developed by extending the theory of micropolar continua to include thermal effects by Eringen [3] and Nowacki [28].

Following various methods, the elastic fields of various loadings, inclusion and inhomogeneity problems, and interaction energy of point defects and dislocation arrangement have been discussed extensively in the past. Generally all materials have elastic anisotropic properties which mean the mechanical behavior of an engineering material is characterized by the direction dependence. However the three dimensional study for an anisotropic material is much more complicated to obtain than the isotropic one, due to the large number of elastic constants involved in the calculation. In particular, transversly isotropic and orthotropic materials, which may not be distinguished from each other in plane strain and plane stress, have been more regularly studied. A review of literature on micropolar orthotropic continua shows that Iesan [10], [11], [12] analysed the static problems of plane micropolar strain of a homogeneous and orthotropic elastic solid, torsion problem of homogeneous and orthotropic cylinders in the linear theory of micropolar elasticity and bending of orthotropic micropolar elastic beams by terminal couple. Nakamura [27] applied finite element method for orthotropic micropolar elasticity. Recently Kumar and Choudhary [17], [18], [19], [20], [21] have discussed various problems in orthotropic micropolar continua.

Because a wide class of crystals such as W, Si, Cu, Ni, Fe, Au, Al etc., which are some frequent by used substances, belong to cubic materials. The cubic materials have nine planes of symmetry whose normals are on the three coordinate axes and on the coordinate planes making an angle $\pi/4$ with the coordinate axes. With the chosen coordinate system along the crystalline directions, the mechanical behavior of a cubic crystal can be characterized by four independent elastic constants A_1, A_2, A_3 and A_4.

Minagawa [25] discussed the propagation of plane harmonic waves in a cubic micropolar medium. Kumar and Rani [22] studied time harmonic sources in a thermally conducting cubic crystal. Recently Kumar and Ailawalia [13], [14] discussed

some source problems in micropolar medium with cubic symmetry.

Kuo [23] and Garg [6] have discussed the problem of inclined load in the theory of elastic solids. Recently, Kumar and Ailawalia [15], [16] studied the response of moving inclined load in micropolar theory of elasticity. The deformation due to other sources such as strip loads, continuous line loads, etc. can also be similarly obtained. The deformation at any point of the medium is useful to analyze the deformation field around mining tremors and drilling into the crust of the earth. It can also contribute to the theoretical consideration of the seismic and volcanic sources since it can account for the deformation fields in the entire volume surrounding the source region. No attempt has been made so far to study the response of inclined load in micropolar thermoelastic medium possessing cubic symmetry.

2. Problem Formulation

We consider a homogeneous, micropolar generalized thermoelastic solid half-space with cubic symmetry. We consider a rectangular coordinate system (x, y, z) having origin on the surface y =0 and y – axis pointing vertically into the medium. Suppose that an inclined line load F_0, per unit length, is acting along the interface on the y – axis and its inclination with z – axis is θ.

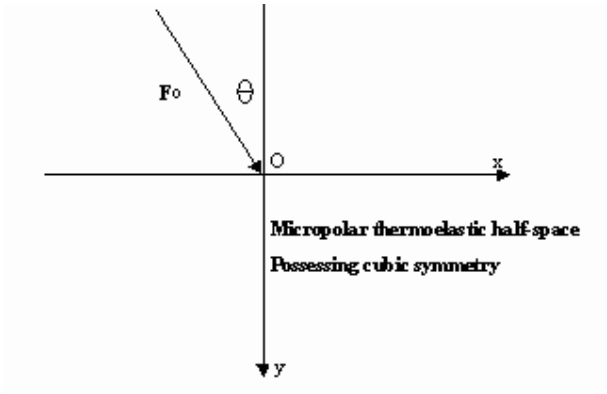

Figure 1

If we restrict our analysis to plane strain parallel to xy – plane with displacement vector $\overrightarrow{u} = (u_1, u_2, 0)$ and microrotation vector $\overrightarrow{\phi} = (0, 0, \phi_3)$ then the field equations and constitutive relations for micropolar thermoelastic solid with cubic symmetry in the absence of body forces, body couples and heat sources can be written by following the equations given by Minagawa [25] and Lord-Shulman [24] as,

$$A_1 \frac{\partial^2 u_1}{\partial x^2} + A_3 \frac{\partial^2 u_1}{\partial y^2} + (A_2 + A_4) \frac{\partial^2 u_2}{\partial x \partial y} + (A_3 - A_4) \frac{\partial \phi_3}{\partial y} - \nu \frac{\partial T}{\partial x} = \rho \frac{\partial^2 u_1}{\partial t^2} \quad (1)$$

$$A_3 \frac{\partial^2 u_2}{\partial x^2} + A_1 \frac{\partial^2 u_2}{\partial y^2} + (A_2 + A_4) \frac{\partial^2 u_1}{\partial x \partial y} - (A_3 - A_4) \frac{\partial \phi_3}{\partial x} - \nu \frac{\partial T}{\partial y} = \rho \frac{\partial^2 u_2}{\partial t^2} \quad (2)$$

$$B_3\nabla^2\phi_3 \; + \; (A_3 - A_4)\left(\frac{\partial u_2}{\partial x} - \frac{\partial u_1}{\partial y}\right) - 2\,(A_3 - A_4)\,\phi_3 = \rho\, j\, \frac{\partial^2\phi_3}{\partial t^2} \tag{3}$$

$$K^*\nabla^2 T = \rho C^*\left(\frac{\partial T}{\partial t} + t_0\frac{\partial^2 T}{\partial t^2}\right) + \nu T_0\left(\frac{\partial}{\partial t} + t_0\frac{\partial^2}{\partial t^2}\right)\left(\frac{\partial u_1}{\partial x} + \frac{\partial u_2}{\partial y}\right) \tag{4}$$

$$t_{22} = A_2\,\frac{\partial u_1}{\partial x} + A_1\,\frac{\partial u_2}{\partial y} - \nu T \tag{5}$$

$$t_{21} = A_4\,\left(\frac{\partial u_2}{\partial x} - \phi_3\right) + A_3\,\left(\frac{\partial u_1}{\partial y} + \phi_3\right) \tag{6}$$

$$m_{23} = B_3\,\frac{\partial \phi_3}{\partial y} \tag{7}$$

where $t_{22}, t_{21},\ m_{23}$ are the components of normal force stress, tangential force stress and tangential couple stress respectively. A_1, A_2, A_3, A_4, B_3 are characteristic constants of the material, $\nu = (A_1 + 2A_2)\,\alpha_T$, α_T is coefficient of linear expansion, ρ is the density and j is the microinertia, K^* is the coefficient of thermal conductivity, C^* is the specific heat at constant strain, t_0 is the thermal relaxation time and $\nabla^2 = \frac{\partial^2}{\partial x^2} + \frac{\partial^2}{\partial y^2}$.

Introducing the dimensionless variables defined by the expressions

$$x' = \frac{\omega^*}{c_1}x, \qquad y' = \frac{\omega^*}{c_1}y, \qquad u_1' = \frac{\rho c_1\omega^*}{\nu T_0}u_1, \qquad u_2' = \frac{\rho c_1\omega^*}{\nu T_0}u_2' \qquad \phi_3' = \frac{\rho c_1^2}{\nu T_0}\phi_3,$$

$$\{t_{22}', t_{21}'\} = \frac{\{t_{22}, t_{21}\}}{\nu T_0}, \qquad m_{23}' = \frac{\omega^*}{c_1\nu T_0}\,m_{23}, \qquad t' = \omega^* t \tag{8}$$

where

$$\omega^{*2} = \frac{\rho C^* c_1^2}{K^*} \quad , \quad c_1^2 = \frac{A_1}{\rho} \tag{9}$$

in equations (1)-(4) we obtain (dropping the primes),

$$\frac{\partial^2 u_1}{\partial x^2} \; + \frac{A_3}{\rho c_1^2}\frac{\partial^2 u_1}{\partial y^2} \; + \frac{(A_2 + A_4)}{\rho c_1^2}\frac{\partial^2 u_2}{\partial x \partial y} \; + \frac{(A_3 - A_4)}{\rho c_1^2}\,\frac{\partial \phi_3}{\partial y} - \frac{\partial T}{\partial x} = \; \frac{\partial^2 u_1}{\partial t^2} \tag{10}$$

$$\frac{A_3}{\rho c_1^2}\frac{\partial^2 u_2}{\partial x^2} \; + \frac{\partial^2 u_2}{\partial y^2} \; + \frac{(A_2 + A_4)}{\rho c_1^2}\frac{\partial^2 u_1}{\partial x \partial y} \; - \frac{(A_3 - A_4)}{\rho c_1^2}\,\frac{\partial \phi_3}{\partial x} - \frac{\partial T}{\partial y} = \; \frac{\partial^2 u_2}{\partial t^2} \tag{11}$$

$$\nabla^2\phi_3 \; + \frac{(A_3 - A_4)\,c_1^2}{B_3\omega^{*2}}\left(\frac{\partial u_2}{\partial x} - \frac{\partial u_1}{\partial y}\right) - \frac{2\,(A_3 - A_4)\,c_1^2}{B_3\omega^{*2}}\phi_3 = \frac{\rho j c_1^2}{B_3}\,\frac{\partial^2\phi_3}{\partial t^2} \tag{12}$$

$$\nabla^2 T = \frac{\rho C^* c_1^2}{K^*\omega^*}\left(\frac{\partial T}{\partial t} + t_0\frac{\partial^2 T}{\partial t^2}\right) + \varepsilon\left(\frac{\partial}{\partial t} + t_0\frac{\partial^2}{\partial t^2}\right)\left(\frac{\partial u_1}{\partial x} + \frac{\partial u_2}{\partial y}\right) \tag{13}$$

Introducing the potential functions defined by

$$u_1 = \frac{\partial q}{\partial x} + \frac{\partial \Psi}{\partial y}\ , \quad u_3 = \frac{\partial q}{\partial y} - \frac{\partial \Psi}{\partial x}\ , \qquad \Psi = -\left(\overrightarrow{U}\right)_y \tag{14}$$

in equations (10)-(13), where $q\,(x,y,t)$ *and* $\Psi\,(x,y,t)$ are scalar potential functions and $\overrightarrow{U}\,(x,y,t)$is the vector potential function we obtain,

$$\left[\frac{\partial^2}{\partial x^2}+a_{11}\frac{\partial^2}{\partial y^2}-\frac{\partial^2}{\partial t^2}\right]q-T=0 \tag{15}$$

$$\left[a_{12}\frac{\partial^2}{\partial x^2}+a_{13}\frac{\partial^2}{\partial y^2}-\frac{\partial^2}{\partial t^2}\right]\Psi+a_{14}\phi_3=0 \tag{16}$$

$$a_{15}\nabla^2\Psi+\left[\nabla^2+2a_{15}-a_{16}\frac{\partial^2}{\partial t^2}\right]\phi_3=0 \tag{17}$$

$$\varepsilon\left[\frac{\partial}{\partial t}+t_0\frac{\partial^2}{\partial t^2}\right]\nabla^2 q+\left[\frac{\partial}{\partial t}+t_0\frac{\partial^2}{\partial t^2}-\nabla^2\right]T=0\,, \tag{18}$$

where

$$a_{11}=\frac{A_2+A_3+A_4}{\rho c_1^2}\,,\quad a_{12}=1-\frac{(A_2+A_4)}{\rho c_1^2}\,,\quad a_{13}=\frac{A_3}{\rho c_1^2}\,,\quad a_{14}=\frac{A_3-A_4}{\rho c_1^2}\,,$$

$$a_{15}=\frac{(A_4-A_3)\,c_1^2}{B_3\omega^{*2}}\,,\quad a_{16}=\frac{\rho j c_1^2}{B_3}\,,\quad \varepsilon=\frac{\nu^2 T_0}{\rho\omega^* K^*} \tag{19}$$

Applying the Laplace transform with respect to time 't' defined by

$$\left\{\overline{q}\,,\ \overline{\Psi}\,,\ \overline{T}\,,\overline{\phi}_3\right\}(x,y,p)=\int_0^\infty\left\{q\,,\ \Psi\,,\ T\,,\phi_3\right\}(x,y,t)\ e^{-pt}\,dt \tag{20}$$

and then the Fourier transform with respect to 'x' defined by

$$\left\{\tilde{q}\,,\ \tilde{\Psi}\,,\ \tilde{T}\,,\tilde{\phi}_3\right\}(\xi,y,p)=\int_{-\infty}^{\infty}\left\{\overline{q}\,,\ \overline{\Psi}\,,\ \overline{T}\,,\overline{\phi}_3\right\}(x,y,p)\ e^{i\xi x}\,dx \tag{21}$$

on equations (15)-(18) and eliminating $\tilde{T}$ and $\tilde{\phi}_3$ from the resulting expressions we get,

$$\left[\frac{d^4}{dy^4}+A^*\frac{d^2}{dy^2}+B^*\right]\tilde{q}=0 \tag{22}$$

$$\left[\frac{d^4}{dy^4}+C^*\frac{d^2}{dy^2}+D^*\right]\tilde{\Psi}=0 \tag{23}$$

where

$$A^*=-\frac{1}{a_{11}}\left[\left(\xi^2+p^2\right)+a_{11}\left(p+t_0p^2+\xi^2\right)+\varepsilon\left(p+t_0p^2\right)\right]$$

$$B^*=\frac{1}{a_{11}}\left[\left(\xi^2+p^2\right)\left(p+t_0p^2+\xi^2\right)+\varepsilon\xi^2\left(p+t_0p^2\right)\right]$$

$$C^*=-\left[\left(\xi^2+a_{16}p^2-2a_{15}\right)+\frac{1}{a_{13}}\left(a_{12}\xi^2+p^2\right)+\frac{a_{14}a_{15}}{a_{13}}\right]$$

$$D^* = \frac{1}{a_{13}}\left[\left(a_{12}\xi^2 + p^2\right)\left(\xi^2 + a_{16}p^2 - 2a_{15}\right) + a_{14}a_{15}\xi^2\right] \tag{24}$$

The roots of equation (21) and (22) are given by

$$q_{1,2}^2 = \frac{-A^* \pm \sqrt{A^{*2} - 4B^*}}{2} \quad q_{3,4}^2 = \frac{-C^* \pm \sqrt{C^{*2} - 4D^*}}{2} \tag{25}$$

The solutions of equations (22) and (23) satisfying radiation conditions are given by

$$\tilde{q} = D_1 \exp\left(-q_1 y\right) + D_2 \exp\left(-q_2 y\right) \tag{26}$$

$$\tilde{\Psi} = D_3 \exp\left(-q_3 y\right) + D_4 \exp\left(-q_4 y\right) \tag{27}$$

$$\tilde{T} = a_1^* D_1 \exp\left(-q_1 y\right) + a_2^* D_2 \exp\left(-q_2 y\right) \tag{28}$$

$$\tilde{\phi_3} = a_3^* D_3 \exp\left(-q_3 y\right) + a_4^* D_4 \exp\left(-q_4 y\right) \tag{29}$$

where

$$\begin{aligned} a_n^* &= a_{11}q_n^2 - \left(\xi^2 + p^2\right) \\ a_\Theta^* &= \frac{1}{a_{14}}\left(a_{12}\xi^2 + p^2 - a_{13}q_\Theta^2\right) \\ n &= 1, 2, \quad \Theta = 3, 4 \end{aligned} \tag{30}$$

3. Boundary Conditions

We consider a normal line load F_1, per unit length acting in the positive y-direction on the interface $y = 0$ along the z – axis and a line force F_2, per unit length acting at the origin in the positive x - direction, then the boundary conditions at the horizontal plane $y = 0$ are,

$$\begin{aligned} t_{22} &= -F_1\psi_1(x)\,\delta(t)\, t_{21} = -F_2\psi_2(x)\ \delta(t) \\ m_{23} &= 0 \quad \frac{\partial T}{\partial y} + hT = 0 \end{aligned} \tag{31}$$

where $\delta(t)$ is Dirac delta function and $\psi_1(x)$ and $\psi_2(x)$ specify the vertical and horizontal traction distribution function along x-axis, h is the heat transfer coefficient where h$\rightarrow \infty$ for isothermal boundary and h $\rightarrow 0$ for insulated boundary.

Applying Laplace and Fourier transform defined by (20) and (21) on the boundary conditions (31) and using (5)-(8), (14) and (26)-(29), we obtain the expressions for displacement components, microrotation, force stress, couple stress and temper-

ature distribution for micropolar thermoelastic solid with cubic symmetry as,

$$\begin{aligned}
\tilde{u}_1 &= -\frac{1}{\Delta}[i\xi\{\Delta_1 \exp(-q_{1y}) + \Delta_2 \exp(-q_{2y})\} \\
&\quad +q_3\Delta_3 \exp(-q_{3y}) + q_4\Delta_4 \exp(-q_{4y})] \qquad (32)\\
\tilde{u_2} &= -\frac{1}{\Delta}[q_1\Delta_1 \exp(-q_{1y}) + q_2\Delta_2 \exp(-q_{2y}) \\
&\quad -i\xi\{\Delta_3 \exp(-q_{3y}) + \Delta_4 \exp(-q_{4y})\}] \qquad (33)\\
\tilde{\phi}_3 &= \frac{1}{\Delta}[a_3^*\Delta_3 \exp(-q_3 y) + a_4^*\Delta_4 \exp(-q_4 y)] \qquad (34)\\
\tilde{t}_{22} &= \frac{1}{\Delta}[r_1\Delta_1 \exp(-q_{1y}) + r_2\Delta_2 \exp(-q_{2y}) \\
&\quad +r_3\Delta_3 \exp(-q_{3y}) + r_4\Delta_4 \exp(-q_{4y})] \qquad (35)\\
\tilde{t}_{21} &= \frac{1}{\Delta}[s_1\Delta_1 \exp(-q_{1y}) + s_2\Delta_2 \exp(-q_{2y}) \\
&\quad +s_3\Delta_3 \exp(-q_{3y}) + s_4\Delta_4 \exp(-q_{4y})] \qquad (36)\\
\tilde{m}_{23} &= -\frac{B_3\omega^2}{\rho c_1^4\Delta}[a_3^*q_3\Delta_3 \exp(-q_3 y) + a_4^*q_4\Delta_4 \exp(-q_4 y)] \qquad (37)\\
\tilde{T} &= \frac{1}{\Delta}[a_1^*\Delta_1 \exp(-q_1 y) + a_2^*\Delta_2 \exp(-q_2 y)] \qquad (38)
\end{aligned}$$

where

$$\begin{aligned}
\Delta &= f_1f_2 - f_3f_4\,, \quad f_1 = s_1g_2^* - s_2g_1^*\,, \quad f_2 = a_3^*q_3r_4 - a_4^*q_4r_3,\\
f_3 &= r_1g_2^* - r_2g_1^*\,, \quad f_4 = a_3^*q_3s_4 - a_4^*q_4s_3, \quad f_5 = a_3^*q_3r_4 - a_4^*q_4r_3 \qquad (39)\\
\Delta_{1,2} &= \pm g_{2,1}^*\left[f_4F_1\tilde{\psi}_1(\xi) - f_5F_2\tilde{\psi}_2(\xi)\right]\\
\Delta_{3,4}^* &= \pm a_{4,3}^*q_{4,3}\left[f_1F_1\tilde{\psi}_1(\xi) - f_3F_2\tilde{\psi}_2(\xi)\right]\\
g_{1,2}^* &= a_{1,2}^*(q_{1,2} - h)\,, \quad r_n = -\xi^2\frac{A_2}{\rho c_1^2} + q_n^2 - a_n^*\\
r_\Theta &= -i\xi q_\Theta\left(1 - \frac{A_2}{\rho c_1^2}\right) \qquad (40)\\
s_n &= i\xi q_n\frac{(A_3 + A_4)}{\rho c_1^2}\,, \quad s_\Theta = \frac{1}{\rho c_1^2}\left[A_3q_\Theta^2 + \xi^2A_4 + (A_3 - A_4)a_\Theta^*\right]\\
n &= 1,2\,; \quad \Theta = 3,4\,. \qquad (41)
\end{aligned}$$

3.1. *Concentrated force*

In order to determine displacements, microrotation, stresses and temperature due to concentrated force described as Dirac delta function $\{\psi_1(x), \psi_2(x)\} = \delta(x)$ must be used with

$$\left\{\tilde{\psi}_1(\xi), \tilde{\psi}_2(\xi)\right\} = 1\,. \qquad (42)$$

3.2. *Uniformly distributed force*

The solution due to the distributed force applied on the half-space is obtained by setting

$$\{\psi_1(x), \psi_2(x)\} = \begin{bmatrix} 1 & if & |x| \le a, \\ 0 & if & |x| > a, \end{bmatrix}$$

in equations (31). The Fourier transform with respect to the pair (x, ξ) for the case of a uniform strip load of unit amplitude and width 2a applied at the origin of the coordinate system $(x = y = 0)$ in dimensionless form after suppressing the primes becomes

$$\left\{\tilde{\psi}_1(\xi), \tilde{\psi}_2(\xi)\right\} = \left[2 \sin\left(\frac{\xi c_1 a}{\omega}\right)/\xi\right], \quad \xi \neq 0. \tag{43}$$

3.3. *Linearly distributed force*

The solution due to linearly distributed force is obtained by substituting

$$\{\psi_1(x), \psi_2(x)\} = \begin{bmatrix} 1 - \frac{|x|}{a} & if & |x| \le a, \\ 0 & if & |x| > a, \end{bmatrix}$$

in equation (31) where 2a is the width of the strip load. The Fourier transform in case of linearly distributed force applied at the origin of the system in dimensionless form is

$$\tilde{\psi}_1(\xi), \tilde{\psi}_2(\xi) = \frac{2\left[1 - \cos\left(\frac{\xi c_1 a}{\omega}\right)\right]}{\frac{\xi^2 c_1 a}{\omega}}. \tag{44}$$

The expressions for displacements, stresses and temperature distribution can be obtained for a concentrated, uniformly and linearly distributed force by replacing $\tilde{\psi}_n(\xi)\,(n = 1, 2)$ from (40)-(42) respectively, in (32)-(38).

4. Particular Cases

Case (4.1): Neglecting micropolarity effect (i.e $B_3 = j = 0$) we obtain the corresponding expressions for displacements, stresses and temperature distribution as,

$$\tilde{u}_1 = -\frac{1}{\Delta^*}\left[i\xi\left\{\Delta_1^* \exp(-q_1 y) + \Delta_2^* \exp(-q_2 y)\right\} + q_3 \Delta_3^* \exp(-q_3' y)\right], \tag{45}$$

$$\tilde{u}_2 = -\frac{1}{\Delta^*}\left[q_1 \Delta_1^* \exp(-q_1 y) + q_2 \Delta_2^* \exp(-q_2 y) - i\xi \Delta_3^* \exp(-q_3' y)\right], \tag{46}$$

$$\tilde{t}_{22} = \frac{1}{\Delta^*}\left[r_1 \Delta_1^* \exp(-q_1 y) + r_2 \Delta_2^* \exp(-q_2 y) + r_3^* \Delta_3^* \exp(-q_3' y)\right], \tag{47}$$

$$\tilde{t}_{21} = \frac{1}{\Delta^*}\left[s_1 \Delta_1^* \exp(-q_1 y) + s_2 \Delta_2^* \exp(-q_2 y) + s_3^* \Delta_3^* \exp(-q_3' y)\right] \tag{48}$$

$$\tilde{T} = \frac{1}{\Delta^*}\left[a_1^* \Delta_1^* \exp(-q_1 y) + a_2^* \Delta_2^* \exp(-q_2 y)\right] \tag{49}$$

where

$$\begin{aligned}
\Delta^* &= g_1^*\left(r_2 s_3^* - r_3^* s_2\right) - g_2^*\left(r_1 s_3^* - r_3^* s_1\right)\\
\Delta_{1,2}^* &= \pm g_{2,1}^*\left[s_3^* F_1 \tilde{\psi}_1(\xi) - r_3^* F_2 \tilde{\psi}_2(\xi)\right]\\
\Delta_3^* &= -F_1\tilde{\psi}_1(\xi)\left(s_1 g_2^* - s_2 g_1^*\right) + F_2\tilde{\psi}_2(\xi)\left(r_1 g_2^* - r_2 g_1^*\right)\\
r_3^* &= -i\xi q_3'\left(1 - \frac{A_2}{\rho c_1^2}\right) s_3^* \;=\; \frac{1}{\rho c_1^2}\left(A_3 q_3^{'2} + \xi^2 A_4\right)\\
q_3^{'2} &= \frac{a_{12}\xi^2 + p^2}{a_{13}}\,.
\end{aligned} \tag{50}$$

Case (4.1a): The expressions for displacements, stresses and temperature can be obtained for a concentrated, uniformly and linearly distributed force by replacing $\tilde{\psi}_n(\xi)\,(n=1,2)$ from (40)-(42) respectively, in (43)-(47).
Case (4.2): Neglecting thermal effect, the expressions for displacements, microrotation and stresses are obtained as,

$$\tilde{u}_1 = -\frac{1}{\Delta^{**}}\left[i\xi\Delta_1^{**}\exp\left(-q_1' y\right) + q_3\Delta_3^{**}\exp\left(-q_3 y\right) + q_4\Delta_4^{**}\exp\left(-q_4 y\right)\right] \tag{51}$$

$$\tilde{u}_2 = -\frac{1}{\Delta^{**}}\left[q_1'\Delta_1^{**}\exp\left(-q_1' y\right) - i\xi\left\{\Delta_3^{**}\exp\left(-q_3 y\right) + \Delta_4^{**}\exp\left(-q_4 y\right)\right\}\right] \tag{52}$$

$$\tilde{\phi}_3 = \frac{1}{\Delta^{**}}\left[a_3^*\Delta_3^{**}\exp\left(-q_3 y\right) + a_4^*\Delta_4^{**}\exp\left(-q_4 y\right)\right] \tag{53}$$

$$\tilde{t}_{22} = \frac{1}{\Delta^{**}}\left[r_1^*\Delta_1^{**}\exp\left(-q_1' y\right) + r_3\Delta_3^{**}\exp\left(-q_3 y\right) + r_4\Delta_4^{**}\exp\left(-q_4 y\right)\right] \tag{54}$$

$$\tilde{t}_{21} = \frac{1}{\Delta^{**}}\left[s_1^*\Delta_1^{**}\exp\left(-q_1' y\right) + s_3\Delta_3^{**}\exp\left(-q_3 y\right) + s_4\Delta_4^{**}\exp\left(-q_4 y\right)\right] \tag{55}$$

$$\tilde{m}_{23} = -\frac{B_3\omega^2}{\rho c_1^4\Delta^{**}}\left[a_3^* q_3\Delta_3^{**}\exp\left(-q_3 y\right) + a_4^* q_4\Delta_4^{**}\exp\left(-q_4 y\right)\right] \tag{56}$$

where

$$\begin{aligned}
\Delta^{**} &= -a_3^* q_3\left(r_1^* s_4 - r_4 s_1^*\right) + a_4^* q_4\left(r_1^* s_3 - r_3 s_1^*\right)\\
\Delta_1^{**} &= -F_1\tilde{\psi}_1(\xi)\left(a_4^* q_4 s_3 - a_3^* q_3 s_4\right) + F_2\tilde{\psi}_2(\xi)\left(a_4^* q_4 r_3 - a_3^* q_3 r_4\right)\\
\Delta_{2,3}^{**} &= \pm a_{4,3}^* q_{4,3}\left[s_1^* F_1\tilde{\psi}_1(\xi) - r_1^* F_2\tilde{\psi}_2(\xi)\right]\\
s_1^* &= i\xi q_1'\frac{\left(A_3 + A_4\right)}{\rho c_1^2}\,,\quad r_1^* \;=\; -\frac{\xi^2 A_2}{\rho c_1^2} + q_1^{'2}\,,\quad q_1^{'2} \;=\; \frac{\xi^2 + p^2}{a_{11}}
\end{aligned} \tag{57}$$

Case (4.2a): Again the expressions for displacements, microrotation, force stress and couple stress can be obtained for a concentrated, uniformly and linearly distributed force by replacing $\tilde{\psi}_n(\xi)\,(n=1,2)$ from (40)-(42) respectively, in (49)-(54).

1: If $h \to 0$, (32)-(38) yields the expressions for displacements, microrotation, stresses and temperature distribution for insulated boundary.

2: If $h \to \infty$, (32)-(38) yields the expressions for displacements, microrotation, stresses and temperature distribution for isothermal boundary.

Case: (4.3) Micropolar thermoelastic solid

Taking $A_1 = \lambda + 2\mu + K$, $A_2 = \lambda$, $A_3 = \mu + K$, $A_4 = \mu$, $B_3 = \gamma$, (56) in equation (32)-(38), (43)-(47) and (49)-(54) with (40)-(42) we obtain the corresponding expressions in micropolar thermoelastic isotropic medium, thermoelastic isotropic medium and micropolar isotropic medium for concentrated, uniformly distributed and linearly distributed force respectively.

5. Inclined line load

For an inclined line load F_0, per unit length, we have (see Figure 1)

$$F_1 = F_0 \cos\theta , \quad F_2 = F_0 \sin\theta . \tag{58}$$

Using (57) in (32)-(38), (43)-(47) and (49)-(54) with (56) and (40)-(42) we obtain the corresponding expressions in micropolar thermoelastic medium possessing cubic symmetry, micropolar thermoelastic isotropic medium, thermoelastic isotropic medium and micropolar isotropic medium for concentrated inclined load, uniformly distributed inclined load and linearly distributed inclined load respectively.

6. Problem II: Moving concentrated normal point load.

We consider a concentrated normal and tangential point load moving along the surface of micropolar thermoelastic solid possessing cubic symmetry in x and y directions respectively. The rectangular cartesian coordinates are introduced having origin on the surface y = 0 and y- axis pointing vertically into the medium. Let us consider a pressure pulse $P(x + Ut)$ which is moving with a constant velocity in the negative x direction for an infinite long time so that a steady state prevails in the neighbourhood of the loading as seen by the observer moving with the load (Figure 2).

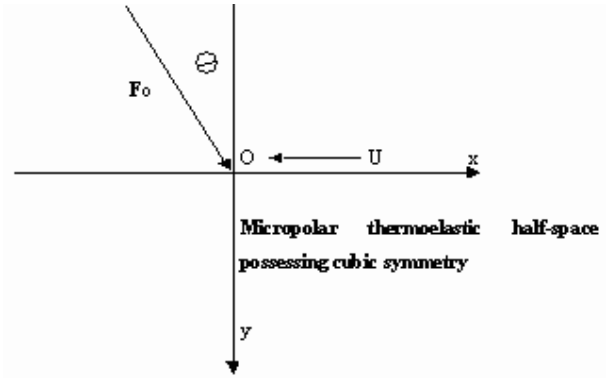

Figure 2

Using Galilean transformations [5] $x^* = x + Ut$, $y^* = y$, $t^* = t$ where U is the magnitude of moving load velocity at the surface of micropolar thermoelastic solid

possessing cubic symmetry and introducing dimensionless quantities defined by

$$x' = \frac{\omega^*}{c_1}x^* \quad , \quad y' = \frac{\omega^*}{c_1}y^*, \quad u_1' = \frac{\rho c_1 \omega^*}{\nu T_0}u_1, \quad u_2' = \frac{\rho c_1 \omega^*}{\nu T_0}u_2, \quad \phi_3' = \frac{\rho c_1^2}{\nu T_0}\phi_3,$$

$$\{t_{22}', t_{21}'\} = \frac{\{t_{22}, t_{21}\}}{\nu T_0}, \quad m_{23}' = \frac{\omega^*}{c_1 \nu T_0}\, m_{23} \tag{59}$$

and applying Fourier transforms defined by (21) in equations (15)-(18), we obtain the results in case of moving load at the surface of micropolar thermoelastic solid possessing cubic symmetry. The boundary conditions in this case are

$$t_{22} = -F_1\,\delta\,(x^*)\ , \quad t_{21} = -F_2\delta\,(x^*)\ , \quad m_{23} = 0\ , \quad \frac{\partial T}{\partial y} + hT = 0$$

The expressions for displacements, microrotation, stresses and temperature distribution for micropolar thermoelastic solid possessing cubic symmetry in case of moving normal and tangential point load are given by (32)-(38) by changing $p^2 \to -\xi^2 \frac{U^2}{c_1^2}$ and $p \to i\xi \frac{U}{c_1}$ in the expressions (24) and $\tilde{\psi}_n\,(\xi)\,(n = 1, 2) \to 1$ in equations (32) and (38).

Introducing (57) in the resulting expressions we obtain the results of moving inclined load on the surface of micropolar thermoelastic medium possessing cubic symmetry.

Similarly we obtain the expressions for moving inclined load in micropolar thermoelastic isotropic medium, thermoelastic isotropic medium and micropolar isotropic medium by introducing the above-mentioned changes.

7. Inversion of the Transform

The transformed displacements and stresses are functions of y, the parameters of Laplace and Fourier transforms *p*and ξ respectively, and hence are of the form $\tilde{f}\,(\xi, y, p)$. To get the function in the physical domain, first we invert the Fourier transform using

$$\begin{aligned} \overline{f}\,(x, y, p) &= \frac{1}{2\pi}\int_{-\infty}^{\infty} e^{-i\xi x}\,\tilde{f}\,(\xi, y, p)\,d\xi \\ &= \frac{1}{\pi}\int_{0}^{\infty} \{\cos\,(\xi x)\,f_e - i\sin\,(\xi x)\,f_o\}\,d\xi \end{aligned} \tag{60}$$

where f_e and f_o are even and odd parts of the function $\tilde{f}\,(\xi, y, p)$ respectively. Thus, expressions (58) give us the transform $\overline{f}\,(x, y, p)$ of the function$f\,(x, y, t)$.

Now, for the fixed values of ξ, x and y, the $\overline{f}\,(x, y, p)$ in the expression (59) can be considered as the Laplace transform $\overline{g}\,(p)$ of some function $g\,(t)$. Following Honig and Hirdes [9], the Laplace transformed function $\overline{g}\,(p)$ can be converted as given below.

The function $g(t)$ can be obtained by using

$$g(t) = \frac{1}{2\pi i} \int_{C-i\infty}^{C+i\infty} e^{pt}\, \overline{g}(p)\, dp, \tag{61}$$

where C is an arbitrary real number greater than all the real parts of the singularities of $\overline{g}(p)$. Taking $p = C + iy$, we get

$$g(t) = \frac{e^{C\,t}}{2\pi} \int_{-\infty}^{\infty} e^{ity}\, \overline{g}(C + iy)\, dy \tag{62}$$

Now, taking $e^{-C\,t}\, g(t)$ as $h(t)$ and expanding it as Fourier series in $[0, 2L]$, we obtain approximately the formula

$$g(t) = g_{\infty}(t) + E_{D'}$$

where

$$g_{\infty}(t) = \frac{C_0}{2} + \sum_{k=1}^{\infty} C_k\ , \quad 0 \le t \le 2L\ , \tag{63}$$

$$C_k = \frac{e^{C\,t}}{L}\, \Re\left[e^{\frac{ik\pi t}{L}}\, \overline{g}\left(C + \frac{ik\pi}{L}\right)\right]\ ,$$

E_D is the discretization error and can be made arbitrary small by choosing C large enough. The value of C and L are chosen according to the criteria outlined by Honig and Hirdes [9].

Since the infinite series in equation (62) can be summed up only to a finite number of N terms, so the approximate value of $g(t)$ becomes

$$g_N(t) = \frac{C_0}{2} + \sum_{k=1}^{N} C_k\ , \quad 0 \le t \le 2L\ , \tag{64}$$

Now, we introduce a truncation error E_T that must be added to the discretization error to produce the total approximation error in evaluating $g(t)$ using the above formula. Two methods are used to reduce the total error. The discretization error is reduced by using the "Korrecktur"- method, Honig and Hirdes [9] and then "ε − algorithm" is used to reduce the truncation error and hence to accelerate the convergence.

The " Korrecktur" –method formula, to evaluate the function $g(t)$ is

$$g(t) = g_{\infty}(t) - e^{-2CL} g_{\infty}(2L + t) + E_{D'}, \tag{65}$$

where

$$|E_{D'}| << |E_D|\ . \tag{66}$$

Thus, the approximate value of $g(t)$ becomes

$$g_{N_k}(t) = g_N(t) - e^{-2CL} g_{N'}(2L + t)\ , \tag{67}$$

where, N' is an integer such that $N' < N$.

We shall now describe the $\varepsilon-$ algorithm which is used to accelerate the convergence of the series in equation (63). Let N be a natural number and $S_m = \sum_{k=1}^{m} C_k$ be the sequence of partial sums of equation (63). We define the $\varepsilon-$sequence by

$$\varepsilon_{0,m} = 0 \ , \quad \varepsilon_{1,m} = S_m \ ,$$

$$\varepsilon_{n+1,m} = \varepsilon_{n-1,m+1} + \frac{1}{\varepsilon_{n,m+1} - \varepsilon_{n,m}}; \quad n, m = 1, 2, 3, ...$$

It can be shown Honig and Hirdes [9] that the sequence $\varepsilon_{1,1}$, $\varepsilon_{3,1}$, ..., $\varepsilon_{N,1}$ converge to $g\,(t) + E_D - C_0/2$ faster than the sequence of partial S_m , $m = 1, 2, 3$.....The actual procedure to invert the Laplace transform reduces to the study of equation (65) together with the $\varepsilon-$ algorithm.

The last step is to evaluate the integral in equation (59). The method for evaluating this integral by Press [29] and which involves the use of Rhomberg's integration with adaptive step size. This, also uses the results from successive refinement of the extended trapezoidal rule followed by extrapolation of the results to the limit when the step size tends to zero.

8. Numerical Results and Discussions

For numerical computations, we take the following values of relevant parameters for micropolar cubic crystal as, $A_1 = 19.6 \times 10^{11}$ [dyne/cm^2]
$A_3 = 5.6 \times 10^{11}$ [dyne/cm^2]
$A_2 = 11.7 \times 10^{11}$ [dyne/cm^2]
$A_4 = 4.3 \times 10^{11}$ [dyne/cm^2]
$B_3 = 0.98 \times 10^{-4}$ [dynes].

For the comparison with micropolar isotropic solid, following Eringen [4] and Dhaliwal and Singh [2], we take the following values of relevant parameters for the case of Magnesium crystal like material as, $\rho = 1.74$ [gm/cm^3]
$\lambda = 9.4 \times 10^{11}$ [dyne/cm^2]
$\mu = 4.0 \times 10^{11}$ [dyne/cm^2]
$K = 1.0 \times 10^{11}$ [dyne/cm^2]
$\gamma = 0.779 \times 10^{-4}$ [dyne]
$j = 0.2 \times 10^{-15}$ [cm^2]
$C^* = 0.104 \times 10^{7}$ [cal/gm^{0}C]
$\nu = 0.0268 \times 10^{9}$ [dyne/cm$^{2\,0}$C]
$T_0 = 23$ [^{0}C]
$K^* = 1.7$ [J/s cm ^{0}C]
$t_0 = 6.131 \times 10^{-13}$ [s]

The values of tangential displacement $U_1 = (u_1/F_0)$, normal displacement $U_2 = (u_2/F_0)$, tangential force stress $T_{21} = (t_{21}/F_0)$ normal force stress $T_{22} = (t_{22}/F_0)$, tangential couple stress $M_{23} = (m_{23}/F_0)$ and temperature distribution $T^* = (T/F_0)$ for a micropolar thermoelastic medium possessing cubic symmetry cubic crystal (MTECC) and micropolar thermoelastic isotropic solid (MTEIS) have been studied and the variations of these components with distance x have been shown by

1. solid line (–) for MTECC and $\theta = 0^0$,
2. dashed line (- -) for MTEIS and $\theta = 0^0$,
3. solid line with centered symbol (x–x–x–x) for MTECC and $\theta = 30^0$,
4. dashed line with centered symbol(x- -x- -x) for MTEIS and $\theta = 30^0$,
5. solid line with centered symbol (o–o–o–o) for MTECC and $\theta = 60^0$,
6. dashed line with centered symbol(o- -o- -o) for MTEIS and $\theta = 60^0$,
7. solid line with centered symbol ($_*--_*--_*--_*$) for MTECC and $\theta = 90^0$,
8. dashed line with centered symbol($_*$- -$_*$- -$_*$) for MTEIS and $\theta = 90^0$.

These variations are shown in Figure 3-26. The computations are carried out for $y = 1.0$ in the range $0 \leq x \leq 10.0$ at $t = 1.0$ and $a = 1.0$ In case of moving inclined load the calculations have been performed for $U < c_1$.

9. Discussions for Various Cases

9.1. *Dynamic Inclined load*

9.1.1. *Concentrated force*

The value of tangential displacement, very close to the point of application of source, increases with increase in the angle of inclination of the source with normal direction. Also for a particular inclination of the source, the values of tangential displacement for MTECC and MTEIS are close to each other. These oscillations are oscillatory in nature and the magnitude of these oscillations decrease with increase in horizontal distance x. These variations of tangential displacement are shown in Figure 3.

Unlike the values obtained for tangential displacement, the values of normal displacement near the point of application of source decreases with increase in the angle of inclination of source with normal direction. But similar to the variations of tangential displacement these variations are oscillatory in nature and their magnitudes decrease with horizontal distance. These variations of normal displacement are shown in Figure 4.

It is observed that the nature of force stress, near the point of application of source, is similar to the nature of displacement components i.e the values of tangential force stress increases whereas the values of normal force stress decreases (at this point). These variations of tangential force stress and normal force stress are shown in Figures 5 and 6 respectively. The variations of both tangential couple stress and temperature distribution increases sharply in the range $0 \leq x \leq 2.0$and then oscillates in the range $2.0 \leq x \leq 10.0$. However the degree of this sharpness decreases with decrease in angle of inclination for tangential couple stress and increase in angle of inclination of the source for temperature distribution. These variations of tangential couple stress and temperature distribution are shown in Figures 7 and 8 respectively.

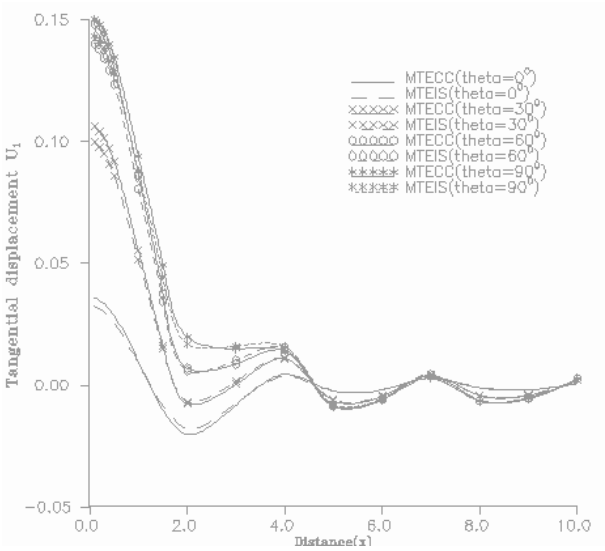

Figure 3 Variation of tangential displacement $U_1 = u_1/F_0$ with distance x. (Concentrated force)

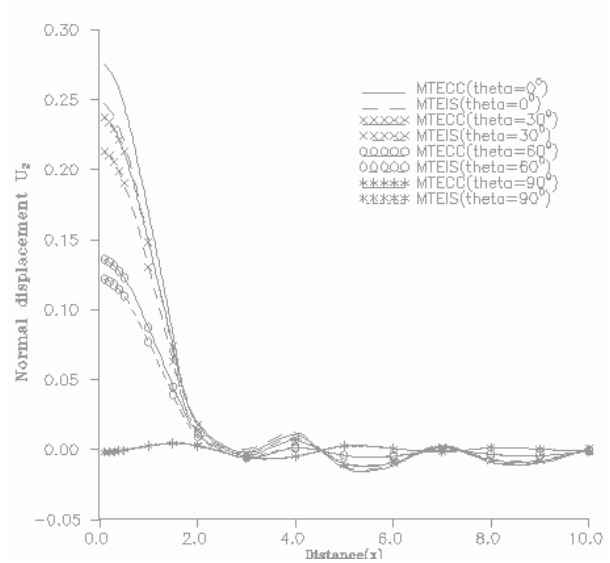

Figure 4 Variation of normal displacement $U_2 = u_2/F_0$ with distance x. (Concentrated force)

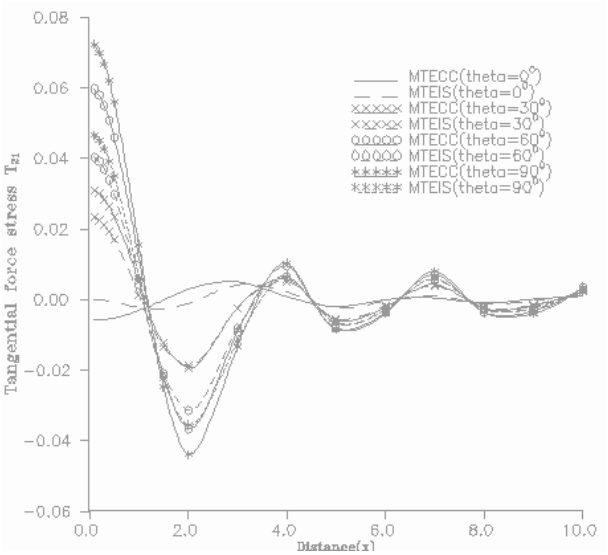

Figure 5 Variation of tangential force stress $T_{21} = t_{21}/F_0$ with distance x. (Concentrated force)

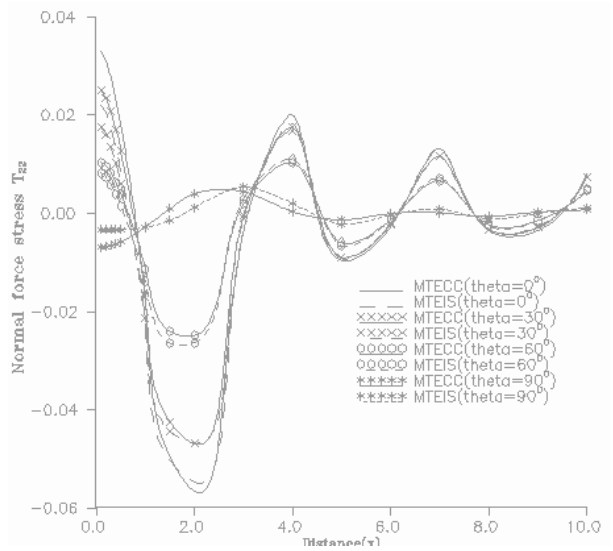

Figure 6 Variation of normal force stress $T_{22} = t_{22}/F_0$ with distance x. (Concentrated force)

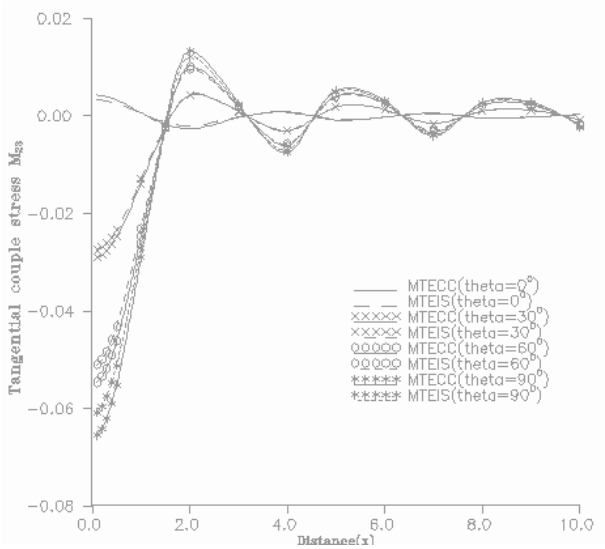

Figure 7 Variation of tangential couple stress $M_{23} = m_{23}/F_0$ with distance x. (Concentrated force)

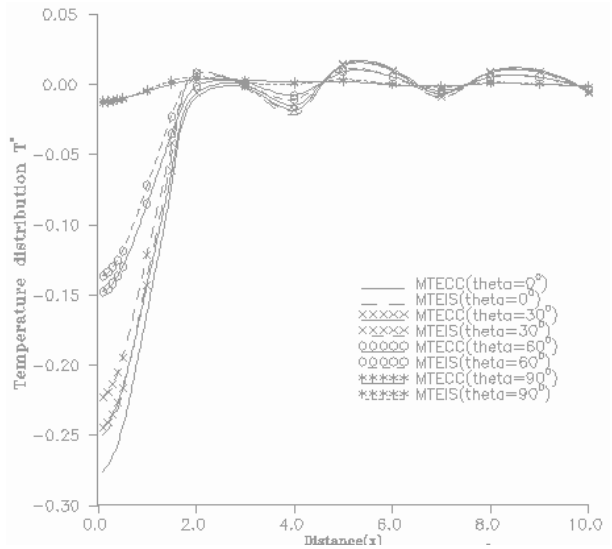

Figure 8 Variation of temperature $T^* = T/F_0$ with distance x. (Concentrated force)

9.1.2. *Uniformly distributed force*

The discussions for displacement components are similar to the discussions given in case of concentrated force. However the variations are similar in nature irrespective of the angle of inclination of source. It is observed that the values of displacement components for both the solids are quite close to each other in the range $6.0 \leq x \leq 10.0$. These variations of tangential displacement and normal displacement on application of uniformly distributed force are shown in Figures 9 and 10 respectively.

The magnitude of oscillations of tangential force stress increases as the source moves from normal to tangential direction. For a particular value of angle of inclination the variations of tangential force stress are more oscillatory for MTECC. These values are of comparable magnitude in the range $6.0 \leq x \leq 10.0$ for MTECC and MTEIS. These variations of tangential force stress are shown in Figure 11. Figure 12 depicts that the values of normal force stress increases sharply when $0 \leq \theta \leq 60^0$ and the degree of this sharpness decreases with increase in angle of inclination of source. Also these values of normal force stress for $\theta = 90^0$lie in a short range as compared to the values when $0 \leq \theta \leq 60^0$.

The variations of tangential couple stress and temperature distribution as shown in Figures 13 and 14 are exactly opposite in nature, with difference in magnitudes, to the variations obtained for tangential displacement and normal displacement on application of uniformly distributed force. The values of tangential couple stress lie in a very short range when $\theta = 0^0$ whereas the values of temperature distribution are in a short range when $\theta = 90^0$ as compared to other values of angle of inclination.

9.1.3. *Linearly distributed force*

The variations of tangential and normal components of a quantity are opposite in nature for a particular value of angle of inclination of the source i.e if the tangential components (displacement or force stress) are less oscillatory then the normal components (displacement or force stress) are more oscillatory for a particular value of θ. It is also observed that the variations of force stress are more oscillatory in nature as compared to the variations of displacement components. These variations of tangential displacement, normal displacement, tangential force stress and normal force stress are respectively shown in Figures 15-18. The variations of tangential couple stress and temperature distribution are exactly opposite in nature to the variations of tangential displacement and normal displacement with difference in magnitudes as was the case discussed on application of uniformly distributed force. These variations of tangential couple stress and temperature distribution are shown in Figures 19 and 20 respectively.

9.2. *Moving Inclined load*

Contrary to the discussions given in case of dynamic inclined load, the variations of tangential displacement and normal displacement are similar in nature to some extent for a given value of angle of inclination. These variations of tangential displacement are a little more oscillatory in nature as compared to the variations of normal displacement. These variations of tangential displacement and normal displacement are shown in Figures 21 and 22 respectively.

The variations of normal force stress are smoother in nature in comparison to the

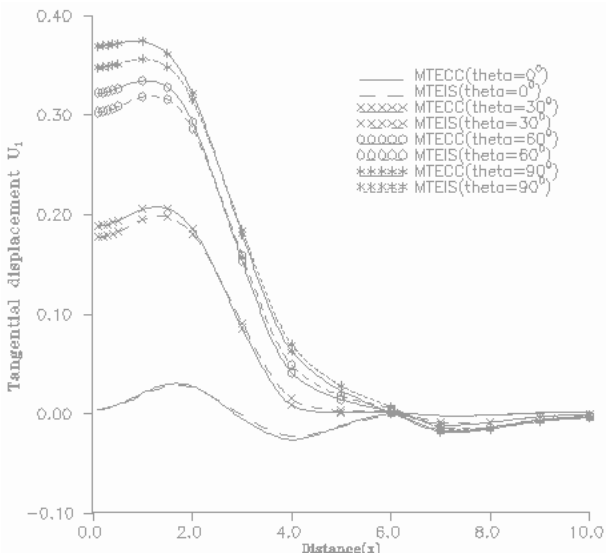

Figure 9 Variation of tangential displacement $U_1 = u_1/F_0$ with distance x. (Uniformly distributed force)

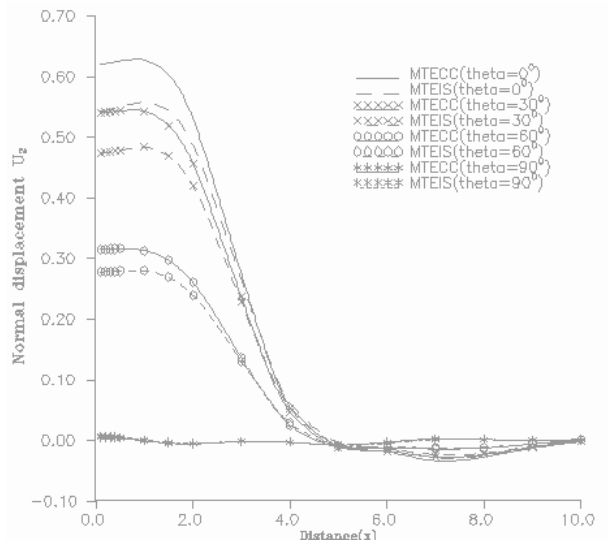

Figure 10 Variation of normal displacement $U_2 = u_2/F_0$ with distance x. (Uniformly distributed force)

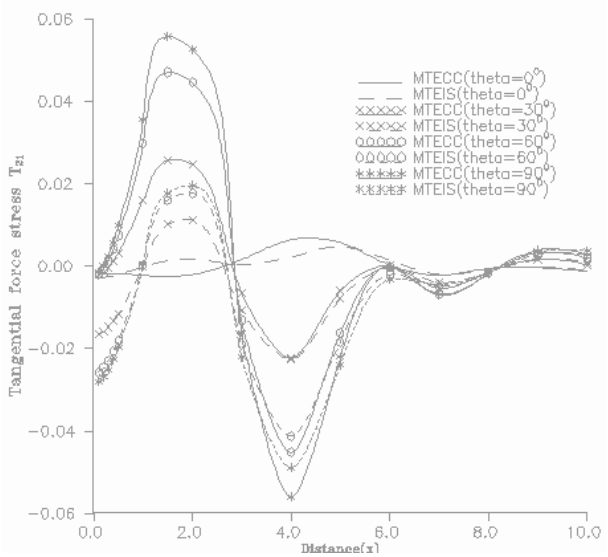

Figure 11 Variation of tangential force stress $T_{21} = t_{21}/F_0$ with distance x. (Uniformly distributed force)

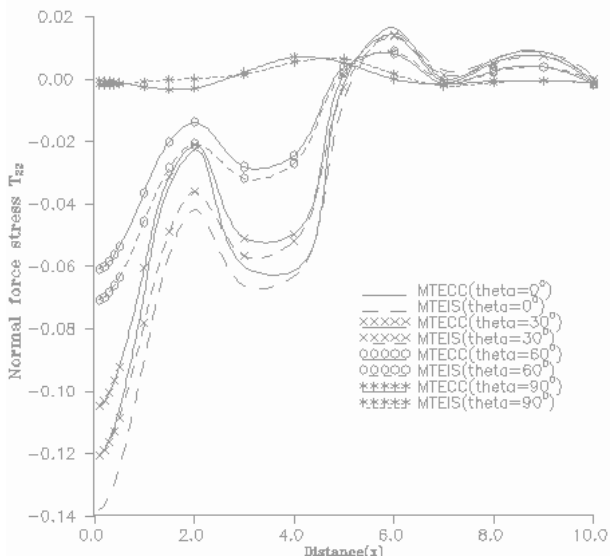

Figure 12 Variation of normal force stress $T_{22} = t_{22}/F_0$ with distance x. (Uniformly distributed force)

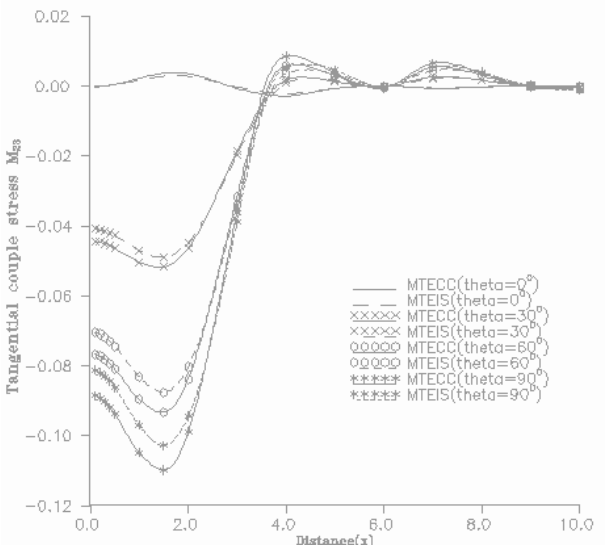

Figure 13 Variation of tangential couple stress $M_{23} = m_{23}/F_0$ with distance x. (Uniformly distributed force)

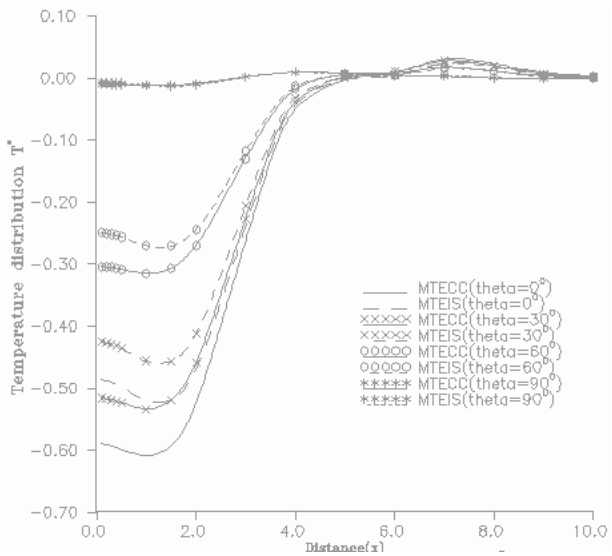

Figure 14 Variation of temperature $T^* = T/F_0$ with distance x. (Uniformly distributed force)

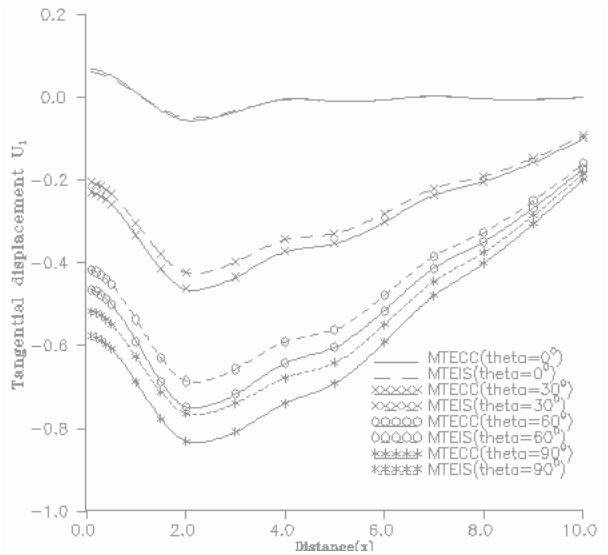

Figure 15 Variation of tangential displacement $U_1 = u_1/F_0$ with distance x. (Lineary distributed force)

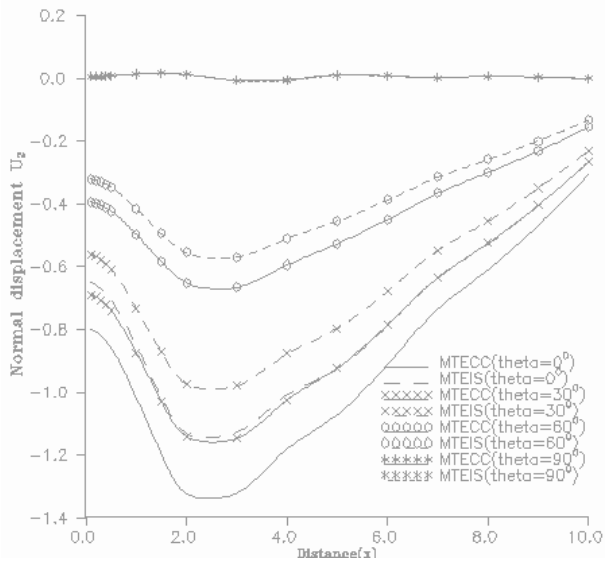

Figure 16 Variation of normal displacement $U_2 = u_2/F_0$ with distance x. (Lineary distributed force)

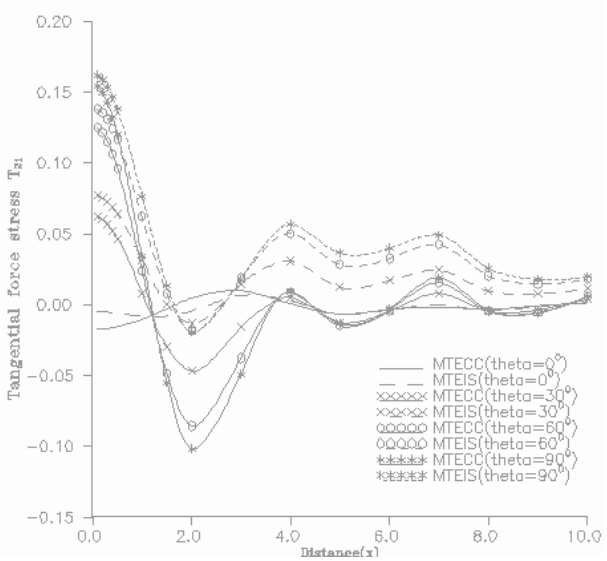

Figure 17 Variation of tangential force stress $T_{21} = t_{21}/F_0$ with distance x. (Lineary distributed force)

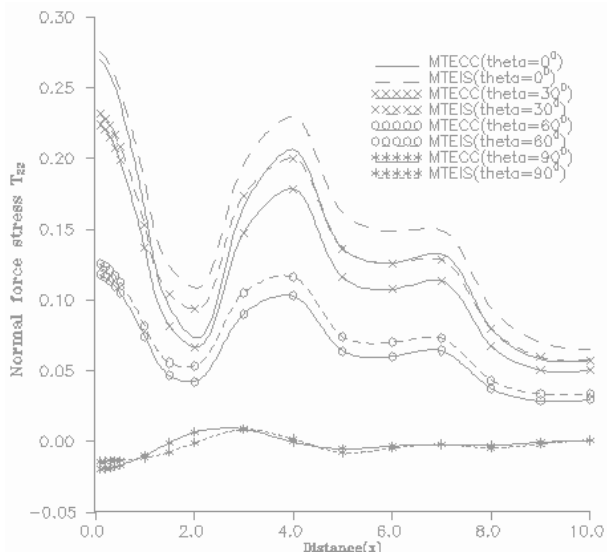

Figure 18 Variation of normal force stress $T_{22} = t_{22}/F_0$ with distance x. (Lineary distributed force)

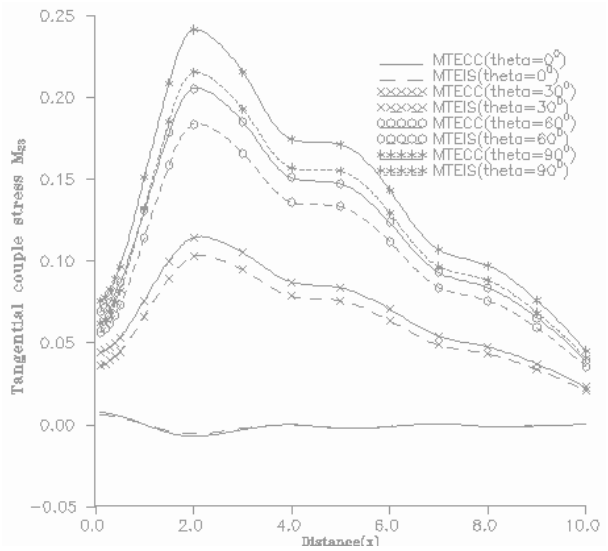

Figure 19 Variation of tangential couple stress $M_{23} = m_{23}/F_0$ with distance x. (Lineary distributed force)

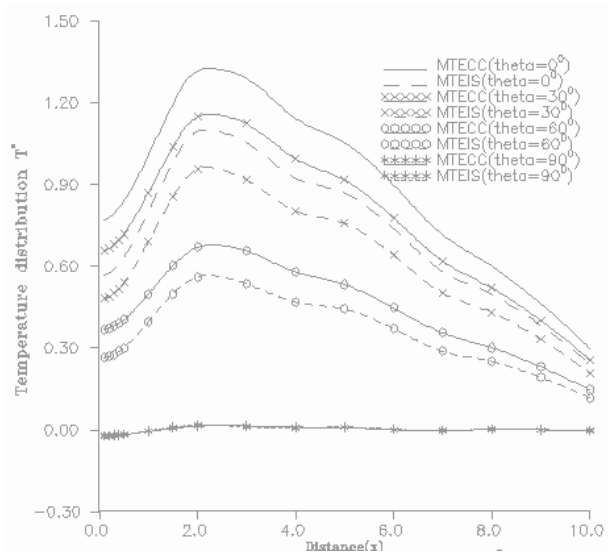

Figure 20 Variation of temperature $T^* = T/F_0$ with distance x. (Lineary distributed force)

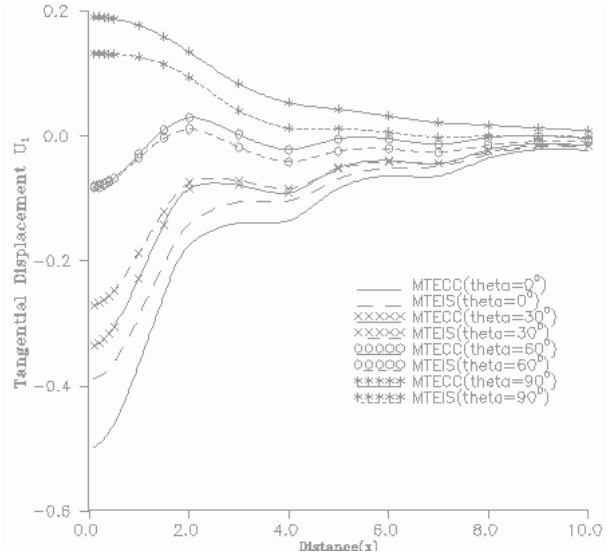

Figure 21 Variation of tangential displacement $U_1 = u_1/F_0$ with distance x

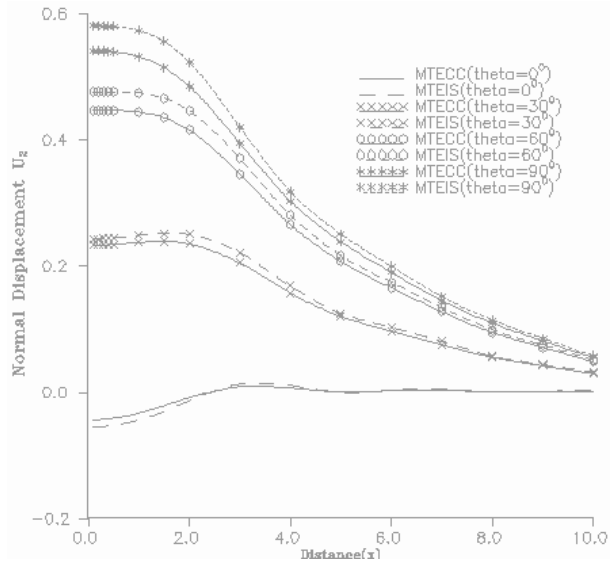

Figure 22 Variation of normal displacement $U_2 = u_2/F_0$ with distance x

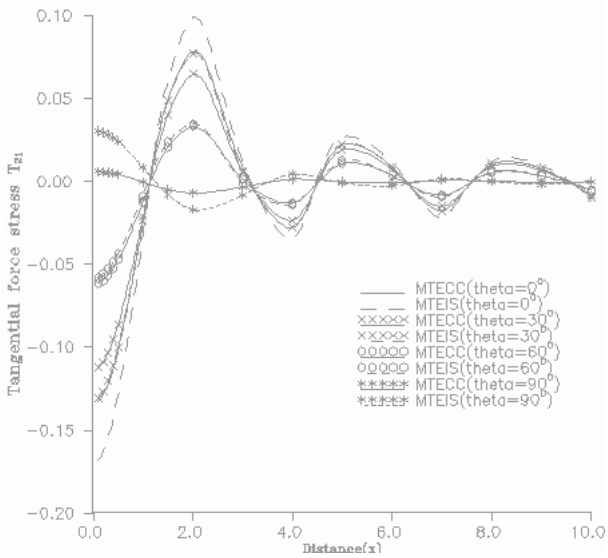

Figure 23 Variation of tangential force stress $T_{21} = t_{21}/F_0$ with distance x

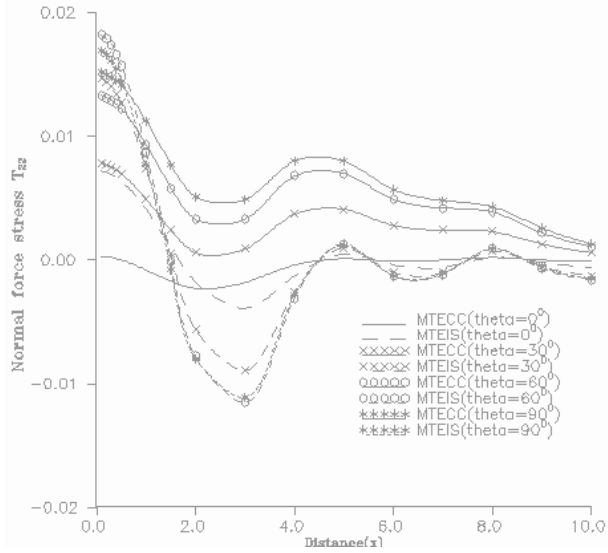

Figure 24 Variation of normal force stress $T_{22} = t_{22}/F_0$ with distance x

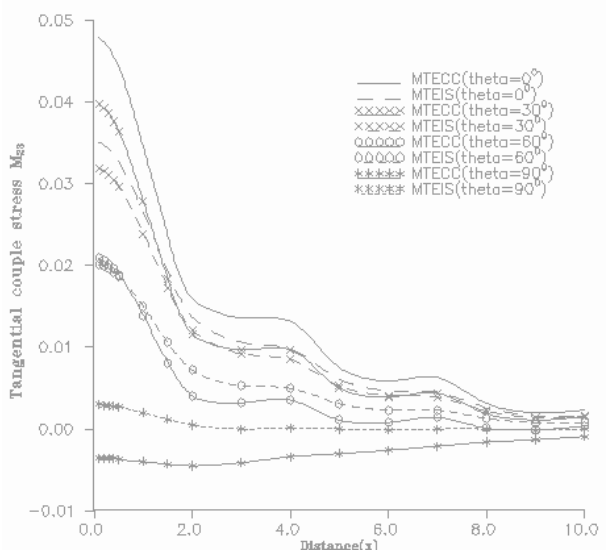

Figure 25 Variation of tangential couple stress $M_{23} = m_{23}/F_0$ with distance x

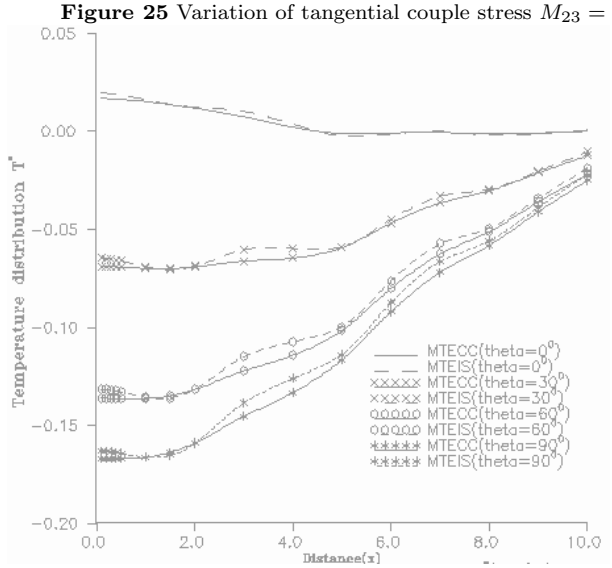

Figure 26 Variation of temperature $T^* = T/F_0$ with distance x

variations of tangential force stress. The difference between the values of tangential force stress for MTECC and MTEIS is very less at any point for a given value of angle of inclination but this difference is quite significant in nature for normal force stress. These variations of tangential force stress and normal force stress when the inclined load is moving on the surface of solid are shown in Figures 23 and 24 respectively.

It is evident from Figure 25 that the values of tangential couple stress for both MTECC and MTEIS decrease, near the point of application of source, as the source moves from normal to tangential direction. The magnitude of these variations also decreases with increase in magnitude of angle of inclination. Figure 26 depicts that the values of temperature distribution for MTECC and MTEIS are very close to each other for a particular direction of application of source.

10. Conclusion

The properties of a body depend largely on the direction of symmetry and the inclination of applied source. When concentrated force is applied on the surface of solid the values of tangential displacement, tangential force stress and temperature distribution increase with increase in angle of inclination of source, near the point of application of source, whereas the values of their normal counterparts decrease at the same points with the same variations. Although the values of a quantity are close to each other for both MTECC and MTEIS for a particular inclination of source yet it is observed that the variations of tangential and normal components of displacement or force stress are opposite in nature for any fixed value of angle of inclination. Unlike the case of dynamic inclined load, when the load is moving on the surface of solid the variations of normal and tangential displacement are similar in nature.

References

[1] **Biot, M.**: Thermoelasticity and irreversible thermodynamics, *J. Appl. Phys.*, 1956, **27**, 240-253.

[2] **Dhaliwal, R S and Singh, A.**: Dynamic coupled Thermoelasticity,*Hindustan Publication Corporation*, New Delhi, India, 1980, p. 726.

[3] **Eringen, A C.**: Foundations of micropolar thermoelasticity course of lectures, CISM Udine, Springer, 1970, **23**.

[4] **Eringen, A C.**: Plane waves in non-local micropolar elasticity. *Int.J.Engg.Sci*, 1984, **22**, 1113-1121.

[5] **Fung Y C.**: Foundations of solid mechanics, *Prentica Hall*, 1968, New, Delhi.

[6] **Garg N R, Kumar R, Goel A and Miglani A.**: Plane strain deformation of an orthotropic elastic medium using eigen value approach, *Earth Planets Space*, 2003, **55**, 3-9.

[7] **Green, A E and Laws, N.**: On the entropy production inequality, *Arch. Ration. Mech. Anal.*, 1972, **45**, 47-53.

[8] **Green, A E and Lindsay, K A.**: Thermoelasticity, *J. Elasticity*, 1972, **2**, 1-5.

[9] **Honig, G. and Hirdes, V.**: A method for the numerical inversion of the Laplace transform, *J.Comp.Appl.Math.*, 1984, **10**, 113-132.

[10] **Iesan, D.**: The plane micropolar strain of orthotropic elastic solids; *Arch. Mech.*, 1973, **25**, 547-561.

[11] **Iesan, D.**: Torsion of anisotropic elastic cylinders, *ZAMM*, 1974, **54**, 773-779.

[12] **Iesan, D.**: Bending of orthotropic micropolar elastic beams by terminal couples, *An .St . Uni . Iasi*, 1974, **20**, 411-418.

[13] **Kumar, R and Ailawalia, P.**: Behaviour of micropolar cubic crystal due to various sources, *Journal of sound and vibration*, 2005, **283**, 3-5, 875-890.

[14] **Kumar, R and Ailawalia, P.**: Deformation in Micropolar cubic crystal due to various sources, *Int. J. Solids. Struct.*, 2005, **42**, 5931-5944.

[15] **Kumar, R and Ailawalia, P.**: Moving inclined load at boundary surface, *Applied Mathematics and Mechanics*, 2005, **26**, No. 4, 76-485.

[16] **Kumar, R and Ailawalia, P.**, Interactions due to inclined load at micropolar elastic half-space with voids, *Int. J. Appl. Mech. Engg.*, , 2005, **10**, No. 1, 109-122.

[17] **Kumar, R and Choudhary, S.**: Influence and Green's function for orthotropic Micropolar continua, *Archives of Mechanics*, 2002, **54**, 185-198.

[18] **Kumar, R and Choudhary, S.**: Dynamical behavior of orthotropic Micropolar elastic medium, *Journal of vibration and Control*, 2002, **8**, 1053-1069.

[19] **Kumar R and Choudhary S.**: Mechanical sources in orthotropic micropolar continua, *Proc. Indian. Acad. Sci(Earth Plant. Sci.)*, 2002, **111**, 2, 133-141.

[20] **Kumar, R and Choudhary, S.**: Response of orthotropic micropolar elastic medium due to various sources, *Meccanica*, 2003, **38**, 349-368.

[21] **Kumar R and Choudhary S.**: Response of orthotropic micropolar elastic medium due to time harmonic sources, *Sadhana* , 2004, Part I **29** 83-92.

[22] **Kumar, R and Rani, L.**: Elastodynamics of time harmonic sources in a thermally conducting cubic crystal, *Int. J. Appl. Mech. Engg.*, 2003, , **8**, No. 4, 637-650.

[23] **Kuo, J T.**: Static response of a multilayered medium under inclined surface loads, *J. Geophysical Research,*, 1969, **74**, No. 12, 3195-3207.

[24] **Lord, H W and Shulman, Y.**: A generalized dynamical theory of thermoelasticity, *J. Mech. Phys. Solids*, 1967, **15**, 299-306.

[25] **Minagawa, S, Arakawa, K, and Yamada, M.**: Dispersion curves for waves in a cubic micropolar medium with reference to Estimations of the Material constants for Diamond. *Bull. JSME.*, 1981, **24**, No. 187, 22-28.

[26] **Műller, J, M.**: The coldness a universal function in thermoelastic bodies,*Arch. Ration. Mech. Anal.*, 1971, **41**, 319-332.

[27] **Nakamura S, Benedict R and Lakes R.**: Finite element method for orthotropic micropolar elasticity ; *Int . J. Engg . Sci*, 1984,**22**, 319-330.

[28] **Nowacki, M.**: Couple-stresses in the theory of thermoelasticity, *Proc. IUTAM Symposia*, Vienna, Editors H, Parkus and L.I Sedov, Springer-Verlag, 1966, 259-278.

[29] **Press, W H., Teukolsky, S A., Vellerling, W T and Flannery, B P.**: Numerical Recipes, *Cambridge: Cambridge University Press*, 1986.

[30] **Suhubi, E S.**: Thermoelastic solids in "A C Eringen(Ed.)", *Continuum Physics*, 1975, **2**, Academic Press, Newyork, Part 2, Chapter 2.